

Error correction for gate operations in systems of exchange-coupled singlet-triplet qubits in double quantum dots

Donovan Buterakos,¹ Robert E. Throckmorton,¹ and S. Das Sarma¹

¹*Condensed Matter Theory Center and Joint Quantum Institute, Department of Physics,
University of Maryland, College Park, Maryland 20742-4111 USA*

(Dated: August 9, 2021)

We present a scheme for correcting for crosstalk- and noise-induced errors in exchange-coupled singlet-triplet semiconductor double quantum dot qubits. While exchange coupling allows the coupling strength to be controlled independently of the intraqubit exchange couplings, there is also the problem of leakage, which must be addressed. We show that, if a large magnetic field difference is present between the two qubits, leakage is suppressed. We then develop pulse sequences that correct for crosstalk- and noise-induced errors and present parameters describing them for the 24 Clifford gates. We determine the infidelity for both the uncorrected and corrected gates as a function of the error-inducing terms and show that our corrected pulse sequences reduce the error by several orders of magnitude.

I. INTRODUCTION

Semiconductor-based electron spin qubits are one of several platforms that are currently being actively investigated, both theoretically and experimentally, with the goal of eventually building a quantum computer. These types of qubits are formed from one or more quantum dots with a single electron trapped inside each. A number of different varieties of semiconductor electron spin qubits exist, such as the single-spin exchange qubit^{1–10}, the singlet-triplet double-dot qubit^{11–20}, the triple-dot exchange-only qubit^{21–25}, and a double-dot “hybrid” qubit with three electrons total^{26–28}. These various spin qubit platforms have been realized in both Si-based and GaAs-based architectures. Other quantum computing platforms include superconducting transmons and trapped ions. While other platforms currently have better coherence times and higher fidelity, allowing a larger number of gates to be performed, semiconductor electron spin qubits allow for faster gates and are compatible with the existing semiconductor industry, thus allowing easier scaling up for eventual real applications beyond just laboratory demonstrations of principles. The greatest challenge for semiconductor-based qubits currently is thus improving coherence time and fidelity. Much progress has been made on this issue, with experiments on singlet-triplet qubits reporting fidelities as high as 99% for single-qubit gates and 90% for two-qubit gates. This still falls short of the goal of at least 99% required to implement surface codes²⁹, let alone the 99.99% fidelity in all operations required before other error-correcting techniques can begin to be implemented. This unfortunately compares unfavorably with superconducting qubits, which claim fidelities of over 99.9% for single-qubit gates and over 99% for two-qubit gates³⁰, and with ion trap qubits, which claim similar fidelities³¹. However, both types of qubits have gate times on the order of μs , compared to ns for semiconductor-based electron spin qubits. The fact that so much experimental progress has been made in semiconductor spin qubits

over the last decade is therefore promising. The subject is currently highly active with around ten large interdisciplinary groups being involved in spin qubit experiments all over the world.

We will focus on the singlet-triplet qubit in this work. These qubits consist of two quantum dots, each with a single electron trapped inside, coupled via exchange coupling and subject to a magnetic field gradient (i.e., magnetic fields that differ at each dot). The exchange coupling can be varied purely electrically, allowing for fast manipulation of the qubit. Typically, the field gradient is created by either depositing a micromagnet nearby or by polarizing the nuclear spins (if possible) and cannot be changed quickly, so it is held constant. However, a recent work³² attempts to realize this gradient electrically by tuning the effective g factor within each quantum dot, which would allow for fast manipulation of this gradient. We will assume, however, that this gradient is held constant, as this is the case in most experiments. We will see later that the form of the effective Hamiltonian for this qubit restricts us to rotations about axes in one quadrant of the xz plane, and furthermore does not allow pure x or z rotations, meaning that rotations about other axes must be performed with complex pulse sequences. Not only does this mean that most rotations require more complex pulse sequences to perform, but also that we cannot implement common error correction schemes such as the NMR-inspired Hahn echo technique or its generalization, the Carr-Purcell-Meiboom-Gill (CPMG) technique^{33–35}. Other techniques are thus required, and have in fact been developed.

We will assume, consistent with the experimental situation, that our qubits are subject to two types of noise—magnetic field noise, present in the field gradient, and charge noise, which manifests as noise in the exchange coupling. We will assume throughout this work that the noise is quasistatic, which is often a good approximation. While the idea of dynamical decoupling in semiconductor spin qubits through specially-designed pulse sequences to improve retention of the qubit state has been around

for years^{18,36–40}, the problem of error correction in the performance of gate operations was first considered in Ref. 41, in which the technique of Soft Uniaxial Positive Control for Orthogonal Drift Error (SUPCODE) was introduced, and further developed in later work^{42,43}. This technique makes use of square pulses (i.e., a piecewise constant J) both to implement gates and to correct errors to arbitrary order. An even more recent work⁴⁴ considers error correction to arbitrary order using smooth pulses, but considers only magnetic field noise.

These works considered singlet-triplet qubits in isolation, without any interqubit coupling. To build a practical quantum computer, one must couple qubits together so that multiqubit gates can be performed as well. The ability to perform arbitrary single-qubit gates and at least one two-qubit gate are necessary for universal quantum computation. The effects of noise on such two-qubit operations has in fact been considered in several works^{42,45–47} (the last of these is actually platform-independent). Such coupling, unfortunately, also introduces a new challenge—crosstalk. The fact that the qubits are coupled means that, while a single-qubit operation is being performed, the changes in the qubit’s state also cause unintended changes in nearby qubits. As a result, we need to correct for crosstalk as well.

There are (at least) two ways to couple singlet-triplet qubits. One method is through capacitive coupling, in which two qubits are coupled via interaction of their dipole moments. The singlet state of a singlet-triplet qubit possesses a nonzero dipole moment, but not the triplet state, resulting in a state-dependent electrostatic interaction. This interaction is empirically found¹⁶ to be proportional to the exchange couplings in the two qubits. Correcting for both noise- and crosstalk-induced error in single-qubit gate operations was the subject of a recent work of ours⁴⁸, which uses a technique based on SUPCODE to cancel errors in single-qubit operations to leading order. The other coupling method, which is also used to couple singlet-triplet qubits, is exchange coupling, in which one of the spins in one qubit is coupled to a spin in the other qubit. This has the advantage of allowing independent control of the intraqubit exchange couplings and the interqubit coupling. However, this also allows for leakage of the system out of the computational subspace; this coupling could, for example, put the system into the state, $|\uparrow\uparrow\downarrow\rangle$. The subject of correcting errors in single-qubit gates performed on one of a pair of exchange-coupled singlet-triplet qubits is the focus of the present work.

The system under consideration is a pair of exchange-coupled singlet-triplet qubits with identical magnetic field gradients, but subject to differing overall magnetic fields. As has been shown, it is not necessary that the magnetic field gradients of the qubits be identical, but we shall assume that they are for simplicity. The differing overall magnetic fields are crucial to allowing us to tune the energy cost of entering the two possible leakage states, $|\uparrow\uparrow\downarrow\rangle$ and $|\downarrow\downarrow\uparrow\rangle$. We split the Hamiltonian

of this system into two parts, one that only connects states within the computational subspace and the magnetic field-induced separation of the leakage states, and those which are responsible for leakage. We then apply perturbation theory to show that a sufficiently large magnetic field can suppress leakage and argue that we can ignore the leakage terms for the remainder of this work. We then outline our approach for developing pulse sequences that correct for noise- and crosstalk-induced errors. This approach is similar to that of Ref. 48, where the case of capacitive interqubit coupling was addressed (in contrast to the current work addressing interqubit exchange coupling). It consists of following the naïve single-qubit gate with identity operations on both qubits arranged in such a way as to cancel the error in the gate to first order. We add these pulses in “blocks” consisting of two pulses on each qubit, arranged such that both pairs have the same duration. This differs from Ref. 48 since, in this previous work, the “blocks” instead consisted of two pulses on one qubit and a single pulse on the other. We find that the arrangement of the “blocks” used in this work allow for shorter pulse sequences, both in time and in number of “blocks” needed. We obtain the parameters needed to correct errors in the naïve pulse sequences introduced in Ref. 43 and show that these sequences reduce the errors (infidelities) in the gates by *several orders of magnitude*. However, we find that, for low noise and low coupling, the error still scales linearly, only transitioning to a quadratic dependence for larger values. This is due to some residual leakage, since we neglect the effect of the terms that cause it. We then point out, however, that the range over which we obtain this linear dependence can be reduced by increasing the magnetic field difference between the qubits.

The rest of the manuscript is organized as follows. Section II introduces the Hamiltonian that we use in the rest of this work and quantifies the magnitude of the effect of leakage out of the computational subspace. In Sec. III, we present the formulas for the first-order error due to crosstalk and noise. Section IV describes the methods that we use to correct for these errors, and we describe our results in Sec. V. We give our conclusions in Sec. VI, and present the detailed numerical parameters for our error-corrected pulse sequences in the Appendix.

II. DERIVATION OF THE HAMILTONIAN

In the singlet-triplet encoding scheme, each qubit is encoded in the spin degrees of freedom of two electrons bound in a pair of quantum dots. An external magnetic field is applied along the z -axis, conserving the z -component of the total spin $S_{1z} + S_{2z}$, and thus the computational space is given by the space with $S_z = 0$. We define the basis states as $|0\rangle = \frac{|\uparrow\downarrow\rangle + |\downarrow\uparrow\rangle}{\sqrt{2}}$, $|1\rangle = \frac{|\uparrow\downarrow\rangle - |\downarrow\uparrow\rangle}{\sqrt{2}}$, though other conventions exist. The effective Hamilto-

nian for a single qubit in this basis is given by

$$H = hX + J(t)Z, \quad (1)$$

where X and Z are the Pauli matrices, h is the magnetic field gradient between the two quantum dots, and J is the exchange coupling. The strength of the magnetic field gradient can only be varied slowly compared to the qubit coherence time, and so we treat h as constant, controlling the qubit only by varying the strength of J . Critically, the sign of J remains the same, meaning that only forward rotations about axes lying in one quadrant of the xz -plane can be performed.

We now consider a system of two singlet-triplet qubits consisting of a linear array of four quantum dots with exchange coupling between nearest neighbors. Other geometries can also be considered, but all will lead to a Hamiltonian of the same basic form. The exchange coupling between the middle two quantum dots serves as a controllable X_1X_2 coupling between the two qubits, allowing for two-qubit gates to be performed⁴⁹. Unfortunately, the presence of this coupling interferes with single qubit operations by introducing crosstalk between the two qubits. While this can be mitigated by simply reducing the strength of the interaction, it can not be entirely eliminated, since the interaction cannot be completely turned off. In addition, for future quantum computing applications with many qubits working together in a circuit, it is essentially impossible to turn off all inter-qubit couplings while performing single qubit operations on specific qubits. This exchange coupling can also potentially introduce leakage outside of the computational subspace. Although the z -component of total spin is still conserved, the mixing of spin states between qubits allows the system to enter, e.g., the state $|\uparrow\uparrow\downarrow\downarrow\rangle$, and conversely. However, leakage can be guarded against by applying a large magnetic field difference between the two ST qubits⁴⁹. We quantify exactly to what degree this protects against leakage by using perturbation theory.

Let us number the spins in one of our qubits 1 and 2, and those in the other qubit 3 and 4. We now add the exchange coupling, $J_{23}\vec{S}_2 \cdot \vec{S}_3$, to the Hamiltonian for the full system, thus coupling the two qubits. We now expand this term out in terms of the x , y , and z components of the spins. The term $J_{23}S_{2z}S_{3z}$ simply allows us to perform two-qubit operations; in terms of our computational basis, this term becomes $\frac{1}{4}J_{23}X_1X_2$. Unfortunately, this is also the term that results in crosstalk between the two qubits. The terms involving the x and y components, on the other hand, cause leakage out of the computational subspace; it is the effect of these terms that we now quantify. In particular, we will show that a large magnetic field difference between the two qubits helps to suppress leakage.

Let B be the energy splitting of each leakage state due to the magnetic field difference between the two qubits. Denote the basis states of the computational subspace by $|n\rangle$, where n runs from 1 to 4, and denote the two leakage states by $|\xi\rangle$, where ξ runs over the two states $|\uparrow\uparrow\downarrow\downarrow\rangle$ and

$|\downarrow\downarrow\uparrow\uparrow\rangle$. Let H_4 denote the terms of the Hamiltonian that connect states within the 4-dimensional computational subspace, and, for simplicity, assume the basis $|n\rangle$ diagonalizes H_4 , so $H_4|n\rangle = E_n|n\rangle$. We let the unperturbed Hamiltonian be given by H_4 plus the terms corresponding to the energies of the leakage states, and we let the perturbation be given by the terms that couple the computational states to the leakage states which we label $k_{n\xi}$ as follows:

$$H_0 = H_4 + B|\uparrow\uparrow\downarrow\downarrow\rangle\langle\uparrow\uparrow\downarrow\downarrow| - B|\downarrow\downarrow\uparrow\uparrow\rangle\langle\downarrow\downarrow\uparrow\uparrow| \quad (2)$$

$$H' = \sum_{n,\xi} k_{n\xi}|\xi\rangle\langle n| + k_{n\xi}^*|n\rangle\langle\xi| \quad (3)$$

The relative energy scales are such that $B \gg E_n \gg k_{n\xi}$. Then using perturbation theory, the leading order corrections to the eigenstates and energies are as follows:

$$|n^1\rangle = \sum_{\xi} \frac{\langle\xi^0|H'|n^0\rangle}{E_n^0 - E_{\xi}^0} |\xi^0\rangle = \sum_{\xi} \frac{k_{n\xi}}{E_n \pm B} |\xi^0\rangle = O\left(\frac{k_{n\xi}}{B}\right) \quad (4)$$

$$E_n^2 = \sum_{\xi} \frac{|\langle\xi^0|H'|n^0\rangle|^2}{E_n^0 - E_{\xi}^0} = \sum_{\xi} \frac{|k_{n\xi}|^2}{E_n \pm B} = O\left(\frac{k_{n\xi}^2}{B}\right) \quad (5)$$

Thus, if a strong magnetic field difference is applied between the two singlet-triplet qubits, the effect of leakage due to exchange coupling is of order k/B . This is sufficiently small to ignore for applications of single-qubit gates, since B can be made large and the value of k is already minimized to reduce crosstalk.

Since a sufficiently large magnetic field difference makes any terms which lead to leakage become negligible, we need only consider the projection of the exchange term $J_{23}\vec{S}_2 \cdot \vec{S}_3$ into the computational space. For simplicity, we define $k = -J_{23}/4$, so that the interaction takes the form kX_1X_2 . Thus the effective Hamiltonian is given by

$$H_4 = h_1X_1 + h_2X_2 + J_1Z_1 + J_2Z_2 + kX_1X_2. \quad (6)$$

III. FIRST ORDER EXPANSIONS OF CROSSTALK AND NOISE

We closely follow the technique developed in Ref. 48, to perform an expansion of the evolution operator e^{-itH} to first order in k . This expansion uses commutation relations of Pauli matrices in order to separate the single-qubit parts of the evolution operator, $e^{-it(h_iX_i + J_iZ_i)}$, from the two-qubit cross terms. To simplify the resulting expressions, we use the shorthand $a_i = \sqrt{h_i^2 + J_i^2}$, and introduce the following rotated basis, chosen so that the single qubit evolution for qubit i reduces to an X'_i rotation.

$$\begin{aligned} X'_i &= (h_iX_i + J_iZ_i)/a_i \\ Y'_i &= Y_i \\ Z'_i &= (-J_iX_i + h_iZ_i)/a_i \end{aligned} \quad (7)$$

This expansion allows the evolution operator to be written in the form

$$e^{-itH} = e^{-it(a_1 X'_1 + a_2 X'_2)} \left(1 - i \sum_{i'j'} \Delta_{i'j'}^{\text{ex}} \sigma_{i'} \otimes \sigma_{j'} \right), \quad (8)$$

where $\sigma_{i'}$ runs over the rotated Pauli matrices X'_1, Y'_1, Z'_1 , and similarly $\sigma_{j'}$ runs over X'_2, Y'_2, Z'_2 . Performing the expansion yields the coefficients $\Delta_{i'j'}^{\text{ex}}$, as follows:

$$\begin{aligned} \Delta_{X'_1 X'_2}^{\text{ex}} &= k \frac{h_1 h_2}{a_1 a_2} t, \\ \Delta_{Y'_1 Y'_2}^{\text{ex}} &= k \frac{J_1 J_2}{2a_1 a_2} \left\{ -t \operatorname{sinc} [2(a_1 + a_2)t] \right. \\ &\quad \left. + t \operatorname{sinc} [2(a_1 - a_2)t] \right\}, \\ \Delta_{Z'_1 Z'_2}^{\text{ex}} &= k \frac{J_1 J_2}{2a_1 a_2} \left\{ t \operatorname{sinc} [2(a_1 + a_2)t] \right. \\ &\quad \left. + t \operatorname{sinc} [2(a_1 - a_2)t] \right\}, \\ \Delta_{X'_1 Y'_2}^{\text{ex}} &= -k \frac{h_1 J_2}{a_1} t^2 \operatorname{sinc}^2 (a_2 t), \\ \Delta_{X'_1 Z'_2}^{\text{ex}} &= -k \frac{h_1 J_2}{a_1 a_2} t \operatorname{sinc} (2a_2 t), \\ \Delta_{Y'_1 Z'_2}^{\text{ex}} &= k \frac{J_1 J_2}{2a_1 a_2} \left\{ (a_1 + a_2) t^2 \operatorname{sinc}^2 [(a_1 + a_2)t] \right. \\ &\quad \left. + (a_1 - a_2) t^2 \operatorname{sinc}^2 [(a_1 - a_2)t] \right\}. \end{aligned} \quad (9)$$

The other three terms ($\Delta_{Y'_1 X'_2}^{\text{ex}}$, $\Delta_{Z'_1 X'_2}^{\text{ex}}$, and $\Delta_{Z'_1 Y'_2}^{\text{ex}}$) are omitted for the sake of brevity, but can be obtained by interchanging the subscripts 1 and 2 in the expressions above. Since J_i is time dependent, the rotated matrices X'_i, Y'_i, Z'_i are also time dependent, and thus are transformed back into the standard basis before proceeding further into the calculation.

In addition to crosstalk, the singlet-triplet qubit system encounters noise from two separate sources, namely, field and charge noise. We work in the quasistatic approximation, where we assume that the noise changes slowly compared to the gate implementation time. These noise sources enter into the Hamiltonian via corrections to the values h_i and J_i . Since the magnetic field itself does not vary over the implementation of the gate, the field noise simply causes a small constant term dh_i to be added to h_i . Charge noise, however, is more subtle, since the value of J_i is changed over the course of the pulse in order to implement each specific gate. If the exchange interaction is adjusted via detuning control, that is, by changing the energy difference ϵ_i between the two dots comprising a qubit, then the change in J_i is given by $dJ_i = \frac{\partial J_i}{\partial \epsilon_i} d\epsilon_i$, where $d\epsilon_i$ is caused by the charge noise and stays constant in the quasistatic limit. Empirically, J_i is found to have an exponential dependence on ϵ_i , at least in the regime of operation, which means that dJ_i is proportional to J_i . It is possible that some systems could have a different dependence of J_i on ϵ_i , but it has

been shown that SUPCODE can easily accommodate these other cases⁴². For specificity, we consider the case of dJ_i being proportional to J_i , i.e., J_i being exponential in ϵ_i .

The expansion of the evolution operator for a single qubit to first order in noise terms has been performed⁵⁰, and since the noise sources as well as the coupling between qubits are small, any effect of one on the other can be ignored. Thus we simply combine the crosstalk expansion terms we obtained with the previously derived noise terms Δ_i^{qn} , so that, to first order, the full noisy evolution operator is given by

$$e^{-itH} = e^{-it(h_1 X_1 + J_1 Z_1)} e^{-it(h_2 X_2 + J_2 Z_2)} \times \left[1 - i \sum_i (\Delta_i^{\text{q1}} \sigma_i \otimes 1 + \Delta_i^{\text{q2}} 1 \otimes \sigma_i) - i \sum_{ij} \Delta_{ij}^{\text{ex}} \sigma_i \otimes \sigma_j \right] \quad (10)$$

with Δ_i^{qn} given by

$$\begin{aligned} \Delta_x^{\text{qn}} &= \frac{2h_n^2 a_n t + J_n^2 \sin 2a_n t}{2a_n^3} dh_n \\ &\quad + \frac{h_n J_n (2a_n t - \sin 2a_n t)}{2a_n^3} dJ_n, \\ \Delta_y^{\text{qn}} &= \frac{J_n (\cos 2a_n t - 1)}{2a_n^2} dh_n \\ &\quad + \frac{h_n (1 - \cos 2a_n t)}{2a_n^2} dJ_n, \\ \Delta_z^{\text{qn}} &= \frac{h_n J_n (2a_n t - \sin 2a_n t)}{2a_n^3} dh_n \\ &\quad + \frac{2J_n^2 a_n t + h_n^2 \sin 2a_n t}{2a_n^3} dJ_n. \end{aligned} \quad (11)$$

The evolution operator given in Eq. (10), is of the form $U = R(1 + \Delta)$, where R is an ideal rotation of qubits 1 and 2 along particular axes of the Bloch sphere, and Δ is some small error produced by noise and crosstalk. Uncorrected rotations along axes in the first quadrant of the xz -plane can be performed simply by allowing the system to evolve at a fixed value of J_1 and J_2 for a given amount of time t . In order to perform rotations about other axes or to correct for crosstalk, it is necessary to perform several uncorrected rotations in a row (i.e., to allow the system to evolve for some time t_1 , then change the values of J_1 and J_2 and allow the system to continue evolving for some time t_2 , etc.). In this case, it is necessary to calculate the errors for each segment of the gate separately and combine the results, since the values of J_1 and J_2 are different for each part. To first order, the result of performing an uncorrected gate U_2 followed by U_1 is

$$U_1 U_2 = R_1 (1 + \Delta_1) R_2 (1 + \Delta_2) = R_1 R_2 (1 + R_2^\dagger \Delta_1 R_2 + \Delta_2). \quad (12)$$

For the pulses we generate, we will set $h_1 = h_2 = h$; however, the same method can be applied to systems where h_1 and h_2 are different. In either case, the noise terms dh_1 and dh_2 are independent.

IV. ERROR CANCELLATION

As with previous SUPCODE pulses, our strategy involves applying an initial uncorrected gate followed by an uncorrected identity operation in such a way that the errors cancel out to leading order. Single qubit rotations have been studied extensively in Ref. 43, so for the initial uncorrected gate, we use the equations presented in that work to generate the desired rotation on qubit 1, and perform a 2π rotation on qubit 2 at the same time. The uncorrected identity operation which follows can be somewhat complex, and in fact, a sufficient degree of complexity is required in order for it to have the freedom to cancel all sources of error for an arbitrary gate. The general form of this identity operation is the key to generating fast, efficient pulse sequences. For a single-qubit system⁴², a sequence of interrupted 2π rotations was used, where the axes of rotation were tuned to precisely cancel out the error. Specifically, the total error of the pulse was calculated in terms of parameters j_n corresponding to the values of J at each part of the gate, and then the total error was set equal to zero, forming a complicated set of equations which were solved numerically for the parameters j_n . Correcting a two-qubit system is significantly more complicated because the amount of time needed to perform 2π rotations differs depending on the axis of rotation, and if qubits 1 and 2 are rotated about different axes concurrently, one operation will finish before the other. Freedom to vary the axes of rotation is needed to allow for numerical solutions which eliminate error, but varying these values can affect the timing between qubits 1 and 2, specifically which segment of the pulse on qubit 1 coincides with a given segment on qubit 2. This makes expressing the total error as a function of a set of parameters, a key step in the error correction process, very difficult.

In order to avoid this problem, Ref. 48 uses a base identity operation consisting of two 2π rotations on one qubit, and a 4π rotation on the other, chosen such that the time taken to perform the 4π rotation equals the total time needed to perform both 2π rotations. While this form of an identity operation solves the problem of timing, it can be somewhat constricting, leading to longer, slower pulses. As stated previously, the major difficulty to performing dynamical decoupling on singlet-triplet qubit systems is the restriction of rotations to the first quadrant of the xz -plane. However, in order to generate efficient pulses, it is necessary to have a large amount of freedom in rotating qubits during the pulse. For singlet-triplet systems, this is best accomplished by allowing sequences with values of J_i alternating between large and small. The scheme that uses a 4π rotation does not allow for strictly alternating values of J_i , since the basic pattern was a nested sequence of 2π , 2π , 4π rotations, corresponding to a cycle between small, large, and medium J_i . Additionally, the value of J_i during the 4π rotation is completely constrained by the parameters chosen for the opposite qubit, meaning that the qubits

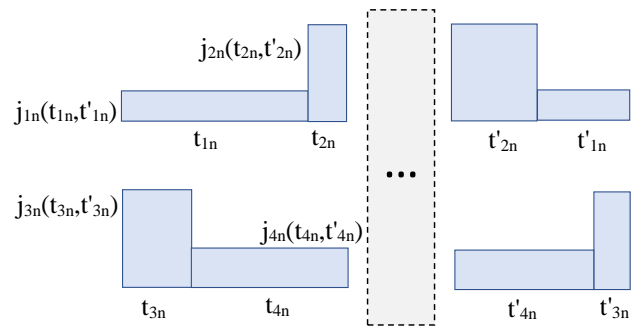


FIG. 1: The base uncorrected identity which consists of two 2π rotations on each qubit (top and bottom). t_{1n} and t'_{1n} define one 2π rotation on qubit 1, and this rotation is interrupted by the 2π rotation given by t_{2n} and t'_{2n} . Similarly, t_{3n} , t'_{3n} , t_{4n} , and t'_{4n} define two 2π rotations on qubit 2. The ellipsis in the middle indicates where copies of this base identity with larger values of n interrupt this identity.

cannot be individually controlled.

We are able to improve upon the previous method by replacing the 4π rotation with two 2π rotations, while still enforcing the constraint that the total time of these two rotations must equal the total time of the two 2π rotations on the other qubit, as shown in the figure (1). This allows an alternating pattern between large and small values of J_i , and reduces the dependence of one qubit's control on the other. To simplify some of the resulting equations, we use the times of each segment of the pulse as the free parameters, rather than the pulse height j_i used in previous works. Ultimately these are equivalent, since for a fixed value of h , the strength of the exchange interaction J_i forms a one-to-one correspondence with the time needed to perform a 2π rotation, as discussed below. We define times t_{1n} through t_{4n} and t'_{1n} through t'_{4n} as in Fig. 1, where the segments of the pulse corresponding to t'_{in} and t'_{in} form a single interrupted 2π rotation. The subscript n distinguishes between the different nested copies of the base identity operation. We impose the constraint that $t_{1n} + t_{2n} = t_{3n} + t_{4n}$, and similarly for t' , meaning that each copy of the base identity has 6 independent parameters. The values of j_{in} are determined in terms of the total time $t_{in} + t'_{in}$ by calculating what value of j_{in} gives a 2π rotation which takes the given amount of time, as follows:

$$j_{in} = \sqrt{\left(\frac{\pi}{t_{in} + t'_{in}}\right)^2 - h^2}. \quad (13)$$

To write the full sequence of operations comprising the nested identity operation, let $U(J_1, J_2, t)$ be an uncorrected rotation at the given values J_1 , and J_2 , for a time t . The sequence of operations before and after the interruption, shown on the left and right of Fig. 1, we denote as A_n and A'_n respectively. These each consist of three rotations: the first and third corresponding to the first

and second 2π rotations on each qubit, and the middle corresponding to the overlap region where part of the first 2π rotation on one qubit is being performed concurrently with the second 2π rotation on the other. This overlap requires a selection statement dependent on which 2π rotations are overlapping, which is determined by the times t_{1n} and t_{3n} . The sequences A_n and A'_n are given by

$$A_n = \begin{cases} U(j_{2n}, j_{4n}, t_{2n})U(j_{1n}, j_{4n}, t_{1n} - t_{3n}) \\ \quad \times U(j_{1n}, j_{3n}, t_{3n}) & \text{if } t_{1n} > t_{3n}, \\ U(j_{2n}, j_{4n}, t_{4n})U(j_{2n}, j_{3n}, t_{3n} - t_{1n}) \\ \quad \times U(j_{1n}, j_{3n}, t_{1n}) & \text{if } t_{1n} < t_{3n}, \end{cases} \quad (14)$$

$$A'_n = \begin{cases} U(j_{1n}, j_{3n}, t'_{3n})U(j_{1n}, j_{4n}, t'_{1n} - t'_{3n}) \\ \quad \times U(j_{2n}, j_{4n}, t'_{2n}) & \text{if } t'_{1n} > t'_{3n}, \\ U(j_{1n}, j_{3n}, t'_{1n})U(j_{2n}, j_{3n}, t'_{3n} - t'_{1n}) \\ \quad \times U(j_{2n}, j_{4n}, t'_{4n}) & \text{if } t'_{1n} < t'_{3n}. \end{cases} \quad (15)$$

We nest multiple copies of the base identity operation in order to create enough degrees of freedom to find a solution that cancels the error of the initial rotation. We find that 5 is the minimum number of copies needed, and so the sequence of rotations which comprise the full uncorrected identity, denoted $I^{(5)}$, is as follows:

$$I^{(5)} = \prod_{n=1}^5 A'_n \prod_{n=5}^1 A_n. \quad (16)$$

The error for each uncorrected rotation is calculated in terms of the parameters t_{in} and t'_{in} by Eq. (10), and added together using Eq. (12), and the result is added to the error of the initial pulse. The norm of this total first order error is numerically minimized over the parameters t_{in} and t'_{in} , and a minimum sufficiently close to zero indicates that the crosstalk and static noise error has been canceled using the pulse sequence given by the values of t_{in} and t'_{in} . Experimental constraints on the value of J_i can be accounted for by defining bounds on the total time of a 2π rotation $t_{\min/\max}$ in terms of the constraining values of $J_{\min/\max}$:

$$t_{\min/\max} = \frac{\pi}{\sqrt{h^2 + J_{\max/\min}^2}}. \quad (17)$$

Then, during the numerical minimization, the constraint on the time for each 2π rotation $t_{\min} < t_{in} + t'_{in} < t_{\max}$ is applied, along with the physical constraint that $t_{in}, t'_{in} > 0$. This ensures that the derived pulse sequence respects experimental limitations. For the pulse sequences we derived, we used values of J_{\min} and J_{\max} equal to $\frac{1}{30}$ and 30 respectively, but other constraints can be used in much the same manner.

V. NUMERICAL RESULTS

We generated pulses which correct against first order error for the 24 Clifford gates. The parameters precisely

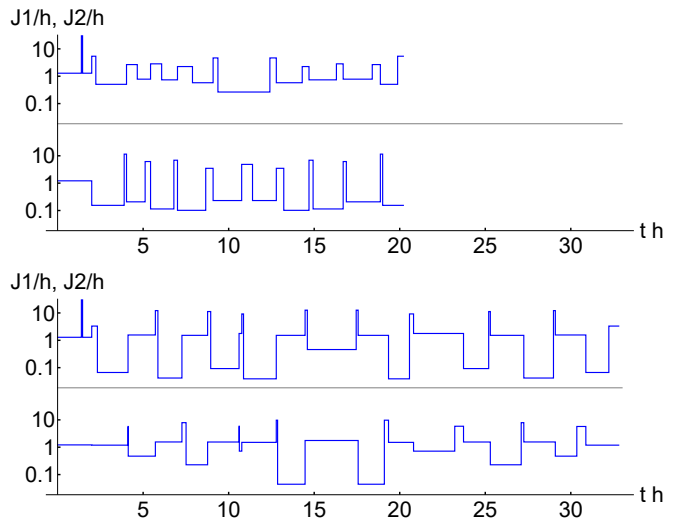


FIG. 2: **Top:** A corrected pulse sequence for the gate $e^{-\frac{2\pi}{3} \frac{X+Y+Z}{\sqrt{3}}}$ using the identity operation presented in this work. **Bottom:** For comparison, a corrected pulse sequence for the same gate using the identity with 4π rotations.

defining these pulses are given in the Appendix. For comparison, we also generated pulses using the previous method which uses 4π rotations. Using the identity operation with two 2π rotations, we are able to reduce the total length of the error correcting identity from 36π to 20π , corresponding to roughly a 40% decrease in the length of the pulse, as shown in figure 2.

A full dynamical decoupling randomized benchmarking analysis is needed to test the pulses against experimental noise. Such an analysis, while feasible, is extremely computationally demanding, and therefore should only be carried out in the context of an actual experimental realization of the pulse sequence developed in the current work. However, we can demonstrate that under a quasistatic noise approximation, the sequences we derived completely cancel first order error. This is done by choosing random values for the errors dh_i/h , dJ_i/J_i and the relative strength of the exchange coupling k/h . From these, the uncorrected rotations performed for each segment of the pulse are evaluated by numerically exponentiating the full 6-dimensional Hamiltonian which includes the noise terms, leakage states, and magnetic field splitting B . By multiplying together the matrices corresponding to each individual segment, the matrix resulting from applying the full pulse with the given noise terms can be found. We denote this matrix $P(dh_i, dJ_i, k)$ and compare it against the ideal Clifford gate which the pulse implements, obtaining a difference Δ_P . The norm of Δ_P , defined as $\sqrt{\text{Tr}(\Delta_P^\dagger \Delta_P)}$, is related to the infidelity of the pulse P averaged over all initial states, and thus is a good measure of total error of the pulse. In order to determine how the error of the pulse scales with initial noise terms, the norm of Δ_P is

plotted against the norm of $(dh_i/h, dJ_i/J_i, k/h)$. In the top portion of Fig. 3, we show such a plot for a value of B equal to $100h$. As shown, the total error is second order for initial error values greater than roughly 10^{-2} , but becomes linear below that point as leakage errors begin to dominate. Increasing or decreasing the value of B will cause this crossover point to shift left or right respectively. One can isolate the behavior of the error in terms of the interaction strength k alone by performing a similar calculation setting dh_i and dJ_i to 0. This shows the error scaling of the corrected and uncorrected pulses more clearly. Specifically, from the bottom of Fig. 3, we again see that the error scales quadratically above 10^{-2} and linearly below that point, yielding an improvement of nearly two orders of magnitude. The reason for the spread in data points in the top graph compared to the bottom, is that for randomly selected noise values, $(dh_i/h, dJ_i/J_i)$ it is possible for different second order error terms to add constructively or destructively, thus adding some variation to the total error of the pulse. Restricting to only one variable produces a much finer line, as this is no longer the case. In both cases, we see the elimination of first order error for noise values above $1/B$.

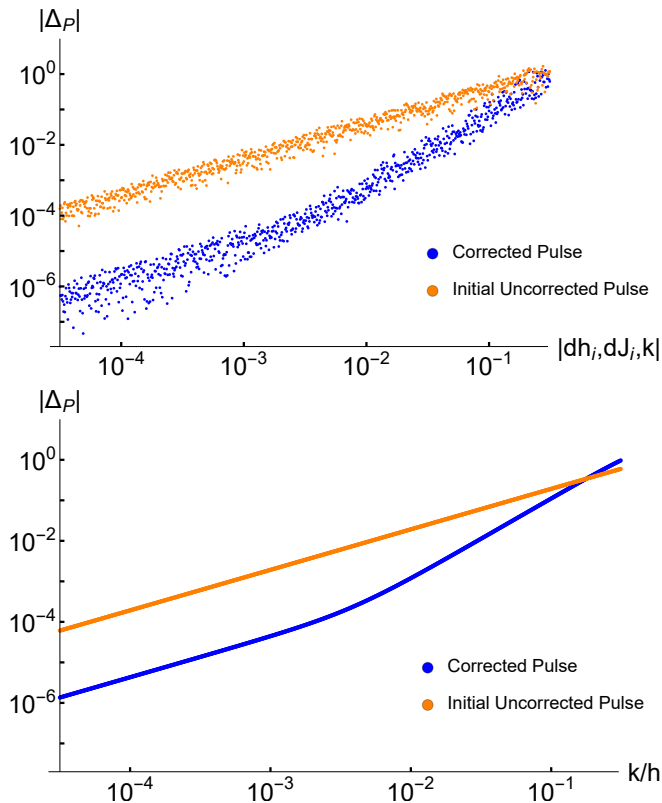


FIG. 3: Error scaling of a naive uncorrected rotation compared with the corrected pulse sequence for the gate $e^{-\frac{2\pi}{3} \frac{X+Y+Z}{\sqrt{3}}}$ at a constant value of $B = 100h$. **Top:** Error with random values of $(dh_i/h, dJ_i/J_i, k/h)$. **Bottom:** Error plotted against only k/h , with $dh_i = dJ_i = 0$.

VI. CONCLUSION

We have demonstrated a method for correcting crosstalk- and noise-induced error in single-qubit gates in exchange-coupled singlet-triplet qubits. Unlike the capacitively-coupled qubits studied in Ref. 48, we can tune the coupling between the qubits independently of the intraqubit exchange coupling used to perform gates. However, leakage out of the computational subspace is a problem here, which does not arise for capacitive coupling. We first showed that a sufficiently large magnetic field difference between the two qubits helps to suppress leakage, and then proceeded to develop pulse sequences that cancel crosstalk- and noise-induced error to first order. Our methods are similar to those used in Ref. 48 for capacitively coupled singlet-triplet qubits—we perform an uncorrected gate, and then follow it with a sequence of uncorrected identity operations designed in such a way as to cancel crosstalk- and noise-induced error in the gate to first order. The basic building blocks of our sequences, however, are different—rather than perform a single 4π rotation on the “idle” qubit, we perform two 2π rotations, each with a different value of the intraqubit exchange coupling. This allows for shorter and faster sequences; we now only require at least 5 of these “blocks”, fewer than what was needed with the older method.

We find that our sequences do, in fact, reduce the error in our qubits by several orders of magnitude. We notice, however, that, for low noise and crosstalk, the error is still first order in our measure of the total error described above, but then crosses over to second-order behavior for larger values. This indicates that, compared to the analogous sequences for capacitively-coupled qubits, our ability to use the sequences presented in this work to combat error is more limited. While, as usual, our results show that reduction of noise and crosstalk during a single-qubit gate are important for improving fidelity, we also show that creating a large magnetic field difference between the two qubits will help to achieve this goal in the case of exchange-coupled qubits. While a number of techniques exist for reducing magnetic field noise, such as polarization of nuclear spins in GaAs or working with isotopically-purified Si, which has very few magnetic impurities, charge noise is much more difficult to handle, in no small part due to the fact that the origin of this noise is poorly understood.

We should also point out that, throughout this work, we made a number of approximations. First of all, we assumed that the magnetic field gradients on the two qubits were the same, which we believe is a reasonable assumption to make. In principle, they could differ, either intentionally or due to natural variation in the field gradients produced at each qubit, whatever the method used to do so might be. Our method already corrects for small, unintentional, variations, since these can essentially be included as part of the noise term. Larger variations, however, would require us to modify our pulse sequences. This also introduces complications similar to

those in the capacitively-coupled case⁴⁸. Second of all, we assumed that the pulses were perfect square pulses. Such pulses are impossible in reality, as there will be a finite rise or fall time. The effect of this finite ramping up or down has been studied in the case of a single isolated qubit⁴², and it was found that the sequences derived therein for correcting noise-induced error still performed well. We thus expect that this will continue to hold true even for the sequences derived in this work. Finally, we assumed that the noise in the system was quasistatic, i.e., it was possible to neglect the time variation in the noise. While this tends to be a good approximation, it is found that, in reality, both types of noise in singlet-triplet qubits exhibit power-law spectra. To be exact, both types of noise follow a $1/f^\alpha$ spectrum, with $\alpha = 2.6$ for the magnetic field noise and 0.7 for the charge noise^{17,51}. Filtering out the high-frequency noise components, especially in the charge noise, will bring a system closer to the quasistatic limit that we worked in. It has been shown, however, that, even in this case, sequences similar to ours for a single isolated qubit^{42,43} still correct errors due to time-dependent noise, and thus we expect the same to hold true for the sequences developed here. Developing a means of combatting noise that takes into full account the time dependence of any specific noise spectrum will likely yield even better results, but doing so is beyond the scope of this work.

Even though we considered the case of two coupled qubits here, an eventual practical quantum computer will have billions of qubits, all with some degree of coupling. As a result, extensions of the techniques developed here to the case of a larger number of qubits will be neces-

sary. Since the coupling between two qubits falls off with distance, we expect that one really only needs to correct for error due to qubits up to a distance of, say, the fifth-nearest neighbors, if that. Correction of errors due to qubits further away should be possible through other error-correction techniques.

Acknowledgments

This work is supported by the Laboratory for Physical Sciences.

Appendix A: Parameters for Dynamical Decoupling Pulse Sequences for the 24 Clifford Gates

In Tables I–III we list parameters defining pulse sequences for the 24 Clifford gates. The top portion of the tables consists of values j_i^{rot} , t_i^{rot} , j'^{rot} which encode the initial rotations as

$$R = \prod_{i=1}^N U(j_i^{\text{rot}}, j'^{\text{rot}}, t_i^{\text{rot}}) \quad (\text{A1})$$

for N equal to 1, 3, or 5, depending on the number of values given in the table. The rest of the tables are the values of t_{in} and t'_{in} which define the uncorrected identity by Eqs. (13)–(16). Only values of i from 1 to 3 are shown with t_{4n} being defined as $t_{1n} + t_{2n} - t_{3n}$, and similarly for t'_{4n} .

¹ D. Loss and D. P. DiVincenzo, Phys. Rev. A **57**, 120 (1998).
² X. Hu and S. Das Sarma, Phys. Rev. A **61**, 062301 (2000).
³ X. Hu and S. Das Sarma, Phys. Rev. A **64**, 042312 (2001).
⁴ K. Nowack, M. Shaffei, M. Laforest, G. E. D. K. Prawiroatmodjo, L. R. Schreiber, C. Reichl, W. Wegscheider, and L. M. K. Vandersypen, Science **333**, 1269 (2011).
⁵ J. J. Pla, K. Y. Tan, J. P. Dehollain, W. H. Lim, J. J. L. Morton, D. N. Jamieson, A. S. Dzurak, and A. Morello, Nature (London) **489**, 541 (2012).
⁶ F. R. Braakman, P. Barthelemy, C. Reichl, W. Wegscheider, and L. M. K. Vandersypen, Nat. Nanotechnol. **8**, **432** (2013).
⁷ J. J. Pla, K. Y. Tan, J. P. Dehollain, W. H. Lim, J. J. L. Morton, F. A. Zwanenburg, D. N. Jamieson, A. S. Dzurak, and A. Morello, Nature (London) **496**, 334 (2013).
⁸ M. Veldhorst, J. C. C. Hwang, C. H. Yang, A. W. Leenstra, B. de Ronde, J. P. Dehollain, J. T. Muhonen, F. E. Hudson, K. M. Itoh, A. Morello, and A. S. Dzurak, Nat. Nanotechnol. **9**, 981 (2014).
⁹ T. Otsuka, T. Nakajima, M. R. Delbecq, S. Amaha, J. Yoneda, K. Takeda, G. Allison, T. Ito, R. Sugawara, A. Noiri, A. Ludwig, A. D. Wieck, and S. Tarucha, Sci. Rep. **6**, 31820 (2016).
¹⁰ T. Ito, T. Otsuka, S. Amaha, M. R. Delbecq, T. Nakajima,

J. Yoneda, K. Takeda, G. Allison, A. Noiri, K. Kawasaki, and S. Tarucha, Sci. Rep. **6**, 39113 (2016).
¹¹ J. Levy, Phys. Rev. Lett. **89**, 147902 (2002).
¹² J. Petta, A. Johnson, J. Taylor, E. Laird, A. Yacoby, M. Lukin, C. Marcus, M. Hanson, and A. Gossard, Science **309**, 2180 (2005).
¹³ S. Foletti, H. Bluhm, D. Mahalu, V. Umansky, and A. Yacoby, Nat. Phys. **5**, 903 (2009).
¹⁴ I. van Weperen, B. D. Armstrong, E. A. Laird, J. Medford, C. M. Marcus, M. P. Hanson, and A. C. Gossard, Phys. Rev. Lett. **107**, 030506 (2011).
¹⁵ B. M. Maune, M. G. Borselli, B. Huang, T. D. Ladd, P. W. Deelman, K. S. Holabird, A. A. Kiselev, I. Alvarado-Rodriguez, R. S. Ross, A. E. Schmitz, M. Sokolich, C. A. Watson, M. F. Gyure, and A. T. Hunter, Nature (London) **481**, 344 (2012).
¹⁶ M. D. Shulman, O. E. Dial, S. P. Harvey, H. Bluhm, V. Umansky, and A. Yacoby, Science **336**, 202 (2012).
¹⁷ O. E. Dial, M. D. Shulman, S. P. Harvey, H. Bluhm, V. Umansky, and A. Yacoby, Phys. Rev. Lett. **110**, 146804 (2013).
¹⁸ M. D. Shulman, S. P. Harvey, J. M. Nichol, S. D. Bartlett, A. C. Doherty, V. Umansky, and A. Yacoby, Nat. Commun. **5**, 5156 (2014).
¹⁹ M. D. Reed, B. M. Maune, R. W. Andrews, M. G. Borselli,

Axis	I	x	x	x	y	y	y	z
Angle	0	$\pi/2$	π	$3\pi/2$	$\pi/2$	π	$3\pi/2$	$\pi/2$
j^{rot}	30.0000	3.37447	1.57530	0.80106	0.82357	0.80164	0.77982	6.50963
j_1^{rot}	30.0000	0.19724	0.19336	0.20358	30.0000	30.0000	30.0000	30.0000
j_2^{rot}	—	30.0000	30.0000	30.0000	0.93548	0.93548	0.93548	6.54409
j_3^{rot}	—	0.19724	0.19336	0.20358	30.0000	30.0000	30.0000	30.0000
j_4^{rot}	—	—	—	—	0.93548	0.93548	0.93548	—
j_5^{rot}	—	—	—	—	30.0000	30.0000	30.0000	—
t_1^{rot}	0.10466	0.39633	0.79278	1.17605	0.02617	0.02617	0.02617	0.01640
t_2^{rot}	—	0.09997	0.09813	0.09981	1.14711	1.14711	1.14711	0.44421
t_3^{rot}	—	0.39633	0.79278	1.17605	0.02617	0.05233	0.07850	0.01640
t_4^{rot}	—	—	—	—	1.14711	1.14711	1.14711	—
t_5^{rot}	—	—	—	—	0.07850	0.07850	0.07850	—
$t_{1,1}$	0.23932	0.52518	0.17782	0.35794	0.87280	1.40951	1.47408	2.08110
$t_{2,1}$	1.09125	1.69460	2.08781	1.29553	0.18612	0.20762	0.35782	0.22124
$t_{3,1}$	1.12263	1.71424	1.94402	1.20225	0.24035	0.28494	0.23108	0.56868
$t'_{1,1}$	0.59780	0.35620	0.40442	0.25259	2.16299	1.40150	1.30849	1.04347
$t'_{2,1}$	1.61793	1.40675	1.05123	1.31383	0.21544	0.48157	0.45315	0.18968
$t'_{3,1}$	1.98543	1.25467	0.69678	1.26393	0.41602	0.17172	0.28890	0.27459
$t_{1,2}$	0.44412	0.30496	0.21167	0.33209	1.80820	1.28984	1.17247	1.28622
$t_{2,2}$	1.43763	1.30979	1.62248	1.40209	0.23931	0.44525	0.33085	0.24893
$t_{3,2}$	1.58580	1.20774	1.51527	1.14195	0.61849	0.19688	0.27989	0.39266
$t'_{1,2}$	0.43189	0.32979	0.22604	0.44226	1.32490	1.43301	1.61739	1.81344
$t'_{2,2}$	1.33166	1.33003	1.32999	1.68187	0.25344	0.24189	0.17401	0.24925
$t'_{3,2}$	1.49696	1.20594	1.39791	1.56451	0.26449	0.19837	0.22329	0.46107
$t_{1,3}$	0.59437	0.19836	0.32108	0.23737	1.63651	1.90912	0.78061	1.32820
$t_{2,3}$	1.27812	1.69950	1.08601	1.62730	0.31245	0.20040	0.99287	0.21810
$t_{3,3}$	1.71539	1.47222	0.47707	1.62737	0.53524	0.39193	0.31686	0.81853
$t'_{1,3}$	0.83936	0.20294	0.25174	0.24861	1.46388	0.77040	0.87515	1.69784
$t'_{2,3}$	0.74344	1.43150	2.03496	1.40707	0.36946	0.94415	0.93132	0.16985
$t'_{3,3}$	1.35372	0.77597	1.92016	0.99473	0.81303	0.36259	0.31753	0.35261
$t_{1,4}$	0.25739	0.22260	0.34850	0.31382	1.76187	1.65753	1.52861	1.27658
$t_{2,4}$	1.59299	1.72292	1.31460	1.94008	0.30317	0.31011	0.21738	0.12688
$t_{3,4}$	1.71721	1.56652	1.04504	1.46824	0.30507	0.22075	0.29048	0.42355
$t'_{1,4}$	0.34269	0.25157	0.26769	0.35810	1.18533	1.19014	1.53603	1.71460
$t'_{2,4}$	1.05712	1.40351	1.82480	1.16347	0.35652	0.43290	0.40722	0.11908
$t'_{3,4}$	1.26890	1.30144	1.54555	1.04779	0.51251	0.25596	0.27451	0.30832
$t_{1,5}$	0.40810	0.12889	0.30221	0.13525	1.93710	1.49564	1.37219	1.31394
$t_{2,5}$	1.78749	1.16500	1.46658	1.36368	0.36629	0.25970	0.25657	0.47911
$t_{3,5}$	1.77536	0.85654	1.49514	1.17617	0.73136	0.29417	0.22679	0.63768
$t'_{1,5}$	0.66870	0.13444	0.31150	0.15842	1.18187	1.43701	1.46942	1.79038
$t'_{2,5}$	1.13501	1.94727	1.26679	1.70282	0.37723	0.19528	0.42305	0.42390
$t'_{3,5}$	1.35550	1.71163	1.36833	1.59387	0.50954	0.32472	0.23331	0.42474

TABLE I: Parameters for the corrected identity, x and y rotations, and z rotation by $\frac{\pi}{2}$.

K. Eng, M. P. Jura, A. A. Kiselev, T. D. Ladd, S. T. Merkel, I. Milosavljevic, E. J. Pritchett, M. T. Rakher, R. S. Ross, A. E. Schmitz, A. Smith, J. A. Wright, M. F. Gyure, and A. T. Hunter, Phys. Rev. Lett. **116**, 110402 (2016).

²⁰ F. Martins, F. K. Malinowski, P. D. Nissen, E. Barnes, S. Fallahi, G. C. Gardner, M. J. Manfra, C. M. Marcus, and F. Kuemmeth, Phys. Rev. Lett. **116**, 116801 (2016).

²¹ D. P. DiVincenzo, D. Bacon, J. Kempe, G. Burkard, and K. B. Whaley, Nature (London) **408**, 339 (2000).

Axis	z	z	$x + y$	$x - y$	$x + z$	$x - z$	$y + z$	$y - z$
Angle	π	$3\pi/2$	π	π	π	π	π	π
j^{rot}	0.36056	0.17551	0.63069	0.63069	2.64575	2.22703	2.30059	2.30059
j_1^{rot}	30.0000	30.0000	0.67417	0.67417	1.00000	30.0000	30.0000	30.0000
j_2^{rot}	0.38039	0.26157	30.0000	30.0000	—	0.87487	0.93444	0.93444
j_3^{rot}	30.0000	30.0000	0.67417	0.67417	—	30.0000	30.0000	30.0000
j_4^{rot}	—	—	—	—	—	—	—	—
j_5^{rot}	—	—	—	—	—	—	—	—
t_1^{rot}	0.02640	0.03937	1.74236	0.86255	1.11072	0.05233	0.02672	0.07794
t_2^{rot}	2.90256	3.01556	0.05233	0.05233	—	1.18222	1.14770	1.14770
t_3^{rot}	0.02640	0.03937	0.86255	1.74236	—	0.05233	0.07794	0.02672
t_4^{rot}	—	—	—	—	—	—	—	—
t_5^{rot}	—	—	—	—	—	—	—	—
$t_{1,1}$	0.99823	1.92843	0.08833	1.28673	0.34596	0.79030	1.60569	0.23302
$t_{2,1}$	0.60853	0.34890	2.00643	0.68412	1.70052	1.81814	0.11982	1.50661
$t_{3,1}$	0.23483	0.72084	1.67281	0.22703	1.56475	2.12906	0.48991	1.26268
$t'_{1,1}$	1.73635	1.20417	0.12953	1.29749	0.37416	0.12950	1.42417	0.59732
$t'_{2,1}$	0.26384	0.39221	1.07374	0.35098	1.41921	1.30677	0.12906	1.52730
$t'_{3,1}$	0.24694	0.24100	0.89230	0.28196	1.37933	0.89247	0.26335	1.65259
$t_{1,2}$	1.61084	1.59488	0.27424	1.42591	0.33335	0.45526	1.58591	0.18225
$t_{2,2}$	0.25952	0.45350	1.48830	0.42358	1.34677	1.44068	0.36992	1.45365
$t_{3,2}$	0.23031	0.13759	1.38719	0.40661	1.21093	1.24880	0.51445	1.25939
$t'_{1,2}$	1.48086	1.52179	0.21616	1.39520	0.34354	0.41969	1.54260	0.18602
$t'_{2,2}$	0.18545	0.34452	1.57898	0.74742	1.61747	1.45752	0.42459	1.46460
$t'_{3,2}$	0.19828	0.77318	1.28815	0.47538	1.28189	1.35509	0.47459	1.25762
$t_{1,3}$	1.31731	1.82596	0.35433	1.29316	0.28838	0.21660	1.39782	0.21928
$t_{2,3}$	0.24558	0.86655	1.35594	0.59180	1.68930	1.46350	0.27381	1.56973
$t_{3,3}$	0.02527	0.91830	0.77629	0.27573	1.34067	0.84143	0.92875	0.98139
$t'_{1,3}$	1.81151	1.28752	0.27864	1.40956	0.25486	0.24862	1.71559	0.21539
$t'_{2,3}$	0.57198	0.69158	1.78281	0.34085	1.37178	1.66983	0.19586	1.56537
$t'_{3,3}$	0.98100	0.66898	1.83730	0.23121	1.02614	1.51736	0.61196	1.08867
$t_{1,4}$	1.39452	0.83871	0.42834	1.16557	0.17440	0.33921	1.39500	0.23414
$t_{2,4}$	0.34113	0.23818	1.37340	0.79534	1.63848	1.34803	0.24753	1.46441
$t_{3,4}$	0.18321	0.20384	1.39414	0.36738	1.45126	1.37034	0.43543	1.39353
$t'_{1,4}$	1.41114	2.28866	0.42670	1.48273	0.23327	0.28588	1.56864	0.24909
$t'_{2,4}$	0.45458	0.12850	1.67357	0.44575	1.47534	1.73744	0.29270	1.45691
$t'_{3,4}$	0.28846	0.33058	1.46928	0.44121	1.26173	1.56477	0.39172	1.42224
$t_{1,5}$	1.63184	1.44467	0.14450	1.34021	0.18444	0.17733	1.29598	0.14930
$t_{2,5}$	0.57060	0.50947	1.57740	0.39524	1.42391	1.37012	0.70988	1.64764
$t_{3,5}$	0.73779	0.26562	1.33720	0.23217	1.18487	0.95442	0.71168	1.33522
$t'_{1,5}$	1.42744	1.51242	0.13516	1.20153	0.17807	0.17531	1.81005	0.16545
$t'_{2,5}$	0.49945	0.44739	1.39521	0.33676	1.69454	1.76074	0.49729	1.43169
$t'_{3,5}$	0.35619	0.65637	1.10140	0.18018	1.50998	1.56945	0.53217	1.17211

TABLE II: Parameters for the dynamically-corrected z rotations by π and $3\pi/2$, and for the rotations by $\hat{x} \pm \hat{y}$, $\hat{x} \pm \hat{z}$, and $\hat{y} \pm \hat{z}$.

Axis	$x+y+z$	$x+y+z$	$-x+y+z$	$-x+y+z$	$x-y+z$	$x-y+z$	$x+y-z$	$x+y-z$
Angle	$2\pi/3$	$4\pi/3$	$2\pi/3$	$4\pi/3$	$2\pi/3$	$4\pi/3$	$2\pi/3$	$4\pi/3$
j^{rot}	1.25195	1.21590	0.26126	0.30530	1.25195	1.21590	0.30530	0.26126
j_1^{rot}	1.28889	1.28889	0.34503	0.34503	1.28889	1.28889	0.34503	0.34503
j_2^{rot}	30.0000	30.0000	30.0000	30.0000	30.0000	30.0000	30.0000	30.0000
j_3^{rot}	1.28889	1.28889	0.34503	0.34503	1.28889	1.28889	0.34503	0.34503
j_4^{rot}	—	—	—	—	—	—	—	—
j_5^{rot}	—	—	—	—	—	—	—	—
t_1^{rot}	1.39062	1.39062	1.16990	1.16990	0.53517	0.53517	1.79990	1.79990
t_2^{rot}	0.03489	0.06977	0.06977	0.03489	0.03489	0.06977	0.03489	0.06977
t_3^{rot}	0.53517	0.53517	1.79990	1.79990	1.39062	1.39062	1.16990	1.16990
t_4^{rot}	—	—	—	—	—	—	—	—
t_5^{rot}	—	—	—	—	—	—	—	—
$t_{1,1}$	1.50682	0.23907	2.09919	2.13904	0.25877	1.32694	0.96335	0.44496
$t_{2,1}$	0.43378	1.79424	0.13944	0.14355	1.37466	0.09653	0.14066	1.19443
$t_{3,1}$	0.36195	1.89588	0.27167	0.24009	1.39970	0.43533	0.15304	1.30631
$t'_{1,1}$	1.42114	0.33431	0.81692	0.88218	0.77381	1.78280	2.05010	0.26043
$t'_{2,1}$	0.60324	1.00912	0.12582	0.11347	1.17007	0.10471	0.14852	1.26224
$t'_{3,1}$	0.48662	1.20899	0.18390	0.22136	1.71261	0.39275	0.70179	1.27329
$t_{1,2}$	1.39992	0.62971	1.49855	1.12516	0.28032	1.86516	1.48547	0.18537
$t_{2,2}$	0.42414	0.77535	0.51557	0.47319	1.74845	0.39374	0.14925	1.52920
$t_{3,2}$	0.27850	1.08828	0.50164	0.16185	1.71345	0.67478	0.30620	1.08443
$t'_{1,2}$	1.21485	0.47335	1.63508	1.99977	0.67062	1.23605	1.64317	0.43359
$t'_{2,2}$	0.42281	1.70063	0.55703	0.44445	1.12901	0.35980	0.23526	1.60726
$t'_{3,2}$	0.22864	1.98788	0.87039	0.90586	1.40689	0.32649	0.34039	1.58324
$t_{1,3}$	0.62378	0.64882	1.66255	1.55661	0.52880	1.27017	1.99104	0.18084
$t_{2,3}$	1.12751	0.92558	0.24453	0.23475	1.32471	0.17439	0.22327	1.80390
$t_{3,3}$	0.27546	1.36298	0.21519	0.61544	1.74611	0.18039	0.44019	1.81096
$t'_{1,3}$	1.86465	0.39490	1.46305	1.56039	0.40115	1.78846	1.06507	0.21559
$t'_{2,3}$	0.19255	1.60297	0.23591	0.22036	1.10171	0.15650	0.22715	1.32750
$t'_{3,3}$	0.41572	1.75840	0.54332	0.17008	1.38539	0.46378	0.25086	0.79889
$t_{1,4}$	1.12639	0.87640	1.58559	1.62250	0.41300	1.68174	1.35793	0.48565
$t_{2,4}$	0.40157	1.20571	0.45452	0.39473	1.29101	0.16459	0.27905	2.07706
$t_{3,4}$	0.29799	1.65093	0.92537	0.31961	1.34976	0.80909	0.05876	1.69366
$t'_{1,4}$	1.72699	0.39587	1.51482	1.50224	0.75062	1.42172	1.63523	0.50811
$t'_{2,4}$	0.40525	1.51421	0.54323	0.32635	1.11254	0.19048	0.20301	1.04977
$t'_{3,4}$	0.23737	1.47462	0.36858	0.74476	1.60877	0.18202	0.61873	1.40129
$t_{1,5}$	1.25033	0.28166	2.10165	2.07986	0.48603	1.22964	1.34488	0.20260
$t_{2,5}$	0.36179	1.76795	0.24481	0.27539	1.22698	0.51213	0.45962	0.96152
$t_{3,5}$	0.24346	1.66999	0.26932	0.44037	1.29670	0.30894	0.57191	0.49989
$t'_{1,5}$	1.57572	0.37654	1.00130	0.99860	0.43093	1.57113	1.65222	0.23722
$t'_{2,5}$	0.32856	1.26919	0.32996	0.31567	1.51202	0.46363	0.33684	2.15458
$t'_{3,5}$	0.25086	1.39094	0.50461	0.40620	1.71000	0.43901	0.22441	2.01752

TABLE III: Parameters for the dynamically-corrected $\hat{x} \pm \hat{y} \pm \hat{z}$ rotations.

²² J. Medford, J. Beil, J. M. Taylor, S. D. Bartlett, A. C. Doherty, E. I. Rashba, D. P. DiVincenzo, H. Lu, A. C. Gossard, and C. M. Marcus, Nat. Nanotechnol. **8**, 654 (2013).

²³ J. Medford, J. Beil, J. M. Taylor, E. I. Rashba, H. Lu, A. C. Gossard, and C. M. Marcus, Phys. Rev. Lett. **111**,

050501 (2013).

²⁴ K. Eng, T. D. Ladd, A. Smith, M. G. Borselli, A. A. Kiselev, B. H. Fong, K. S. Holabird, T. M. Hazard, B. Huang, P. W. Deelman, I. Milosavljevic, A. E. Schmitz, R. S. Ross, M. F. Gyure, and A. T. Hunter, Sci. Adv. **1**, e1500214

- (2015).
- ²⁵ Y.-P. Shim and C. Tahan, *Phys. Rev. B* **93**, 121410(R) (2016).
 - ²⁶ Z. Shi, C. B. Simmons, J. R. Prance, J. K. Gamble, T. S. Koh, Y.-P. Shim, X. Hu, D. E. Savage, M. G. Lagally, M. A. Eriksson, M. Friesen, and S. N. Coppersmith, *Phys. Rev. Lett.* **108**, 140503 (2012).
 - ²⁷ D. Kim, Z. Shi, C. B. Simmons, D. R. Ward, J. R. Prance, T. S. Koh, J. K. Gamble, D. E. Savage, M. G. Lagally, M. Friesen, S. N. Coppersmith, and M. A. Eriksson, *Nature (London)* **511**, 70 (2014).
 - ²⁸ D. Kim, D. R. Ward, C. B. Simmons, D. E. Savage, M. G. Lagally, M. Friesen, S. N. Coppersmith, and M. A. Eriksson, *npj Quant. Inf.* **1**, 15004 (2015).
 - ²⁹ A. G. Fowler, M. Mariantoni, J. M. Martinis, A. N. Cleland, *Phys. Rev. A* **86**, 032324 (2012).
 - ³⁰ R. Barends, J. Kelly, A. Megrant, A. Veitia, D. Sank, E. Jeffrey, T. C. White, J. Mutus, A. G. Fowler, B. Campbell, Y. Chen, Z. Chen, B. Chiaro, A. Dunsworth, C. Neill, P. O'Malley, P. Roushan, A. Vainsencher, J. Wenner, A. N. Korotkov, A. N. Cleland, and J. M. Martinis, *Nature* **508**, 500 (2014).
 - ³¹ J. Benhelm, G. Kirchmair, C. F. Roos, and R. Blatt, *Nat. Phys.* **4**, 463 (2008).
 - ³² P. Harvey-Collard, R. M. Jock, N. T. Jacobson, A. D. Baczewski, A. M. Mounce, M. J. Curry, D. R. Ward, J. M. Anderson, R. P. Manginell, J. R. Wendt, M. Rudolph, T. Pluym, M. P. Lilly, M. Pioro-Ladrière and M. S. Carroll, *IEEE International Electron Devices Meeting (IEDM)*, 36.5.1-36.5.4 (2017).
 - ³³ W. M. Witzel and S. Das Sarma, *Phys. Rev. Lett.* **98**, 077601 (2007).
 - ³⁴ W. M. Witzel and S. Das Sarma, *Phys. Rev. B* **76**, 241303 (2007).
 - ³⁵ B. Lee, W. M. Witzel, and S. Das Sarma, *Phys. Rev. Lett.* **100**, 160505 (2008).
 - ³⁶ H. Bluhm, S. Foletti, D. Mahalu, V. Umansky, A. Yacoby, *Phys. Rev. Lett.* **105**, 216803 (2010).
 - ³⁷ H. Bluhm, S. Foletti, I. Neder, M. Rudner, D. Mahalu, V. Umansky, and A. Yacoby, *Nat. Phys.* **7**, 109 (2011).
 - ³⁸ A. Sergeevich, A. Chandran, J. Combes, S. D. Bartlett, and H. M. Wiseman, *Phys. Rev. A* **84**, 052315 (2011).
 - ³⁹ J. T. Muhonen, J. P. Dehollain, A. Laucht, F. E. Hudson, T. Sekiguchi, K. M. Itoh, D. N. Jamieson, J. C. McCallum, A. S. Dzurak, and A. Morello, *Nat. Nanotechnol.* **9**, 986 (2014).
 - ⁴⁰ F. T. Malinowski, F. Martins, P. D. Nissen, E. Barnes, L. Cywiński, M. S. Rudner, S. Fallahi, G. C. Gardner, M. J. Manfra, C. M. Marcus, and F. Kuemmeth, *Nat. Nanotechnol.* **12**, 16 (2017).
 - ⁴¹ X. Wang, L. S. Bishop, J. P. Kestner, E. Barnes, K. Sun, and S. Das Sarma, *Nat. Commun.* **3**, 997 (2012).
 - ⁴² X. Wang, L. S. Bishop, E. Barnes, J. P. Kestner, and S. Das Sarma, *Phys. Rev. A* **89**, 022310 (2014).
 - ⁴³ R. E. Throckmorton, C. Zhang, X.-C. Yang, X. Wang, E. Barnes, and S. Das Sarma, *Phys. Rev. B* **96**, 195424 (2017).
 - ⁴⁴ J. Zeng, X.-H. Deng, A. Russo, and E. Barnes, *New J. Phys.* **20**, 033011 (2018).
 - ⁴⁵ Y.-L. Wu and S. Das Sarma, *Phys. Rev. B* **96**, 165301 (2017).
 - ⁴⁶ X. Wang, E. Barnes, and S. Das Sarma, *npj Quant. Inf.* **1**, 15003 (2015).
 - ⁴⁷ F. A. Calderon-Vargas and J. P. Kestner, *Phys. Rev. Lett.* **118**, 150502 (2017).
 - ⁴⁸ D. Buterakos, R. E. Throckmorton, and S. Das Sarma, *Phys. Rev. B* **97**, 045431 (2018).
 - ⁴⁹ R. Li, X. Hu, and J. Q. You, *Phys. Rev. B* **86**, 205306 (2012).
 - ⁵⁰ J. P. Kestner, X. Wang, L. S. Bishop, E. Barnes, and S. Das Sarma, *Phys. Rev. Lett.* **110**, 140502 (2013).
 - ⁵¹ J. Medford, L. Cywiński, C. Barthel, C. M. Marcus, M. P. Hanson, and A. C. Gossard, *Phys. Rev. Lett.* **108**, 086802 (2012).